Transient Changes in Four GLUT4 Compartments in Rat Adipocytes during the Transition, Insulin-Stimulated To Basal: Implications for the GLUT4 Trafficking Pathway†

J. S. Hah,‡ J. W. Ryu, W. Lee,§ B. S. Kim, M. Lachaal, R. A. Spangler, and C. Y. Jung*

Department of Physiology and Biophysics, State University of New York at Buffalo, School of Medicine and Biomedical Sciences, and VA Medical Center, Medical Research Service, Buffalo, New York 14215

Received July 17, 2002; Revised Manuscript Received September 25, 2002

ABSTRACT: In rat adipocytes, insulin-induced GLUT4 recruitment to the plasma membrane (PM) is associated with characteristic changes in the GLUT4 contents of three distinct endosomal fractions, T, H, and L. The organelle-specific marker distribution pattern suggests that these endosomal GLUT4 compartments are sorting endosomes (SR), GLUT4-storage endosomes (ST), and GLUT4 exocytotic vesicules (EV), respectively, prompting us to analyze GLUT4 recycling based upon a four-compartment kinetic model. Our analysis revealed that insulin modulates GLUT4 trafficking at multiple steps, including not only the endocytotic and exocytotic rates, but also the two rate coefficients coupling the three intracellular compartments. This analysis assumes that GLUT4 cycles through PM T, H,L, and back to PM, in that order, with transitions characterized by four first-order coefficients. Values assigned to these coefficients are based upon the four steady-state GLUT4 pool sizes assessed under both basal and insulin stimulated states and the transition time courses observed in the plasma membrane GLUT4 pool. Here we present the first reported experimental measurements of transient changes in each of the four GLUT4 compartments during the insulin-stimulated to basal transition in rat adipocytes and compare these experimental results with the corresponding model simulations. The close correlation of these results offers clear support for the general validity of the assumed model structure and the assignment of the T compartment to the sorting endosome GLUT4 pool. Variations in the recycling pathway from that of an unbranched cyclic topography are also considered in the light of these experimental observations. The possibility that H is a coupled GLUT4 storage compartment lying outside the direct cyclic pathway is contraindicated by the data. Okadaic acid-induced GLUT4 recruitment is accompanied by modulation of the rate coefficients linking individual endosomal GLUT4 compartments, further demonstrating a significant role of the endosomal pathways in GLUT4 exocytosis.

GLUT4[1] in rat adipocytes resides mostly in intracellular sites in the basal state, while cellular insulin treatment causes GLUT4 redistribution, leading to a drastic increase in the plasma membrane GLUT4 level (*1*, *2*). GLUT4 in these cells is also known to constantly and rapidly recycle between the plasma membrane and the intracellular sites (*3*, *4*), via endocytosis, exocytosis, and endosomal trafficking involving multiple, morphologically distinct, subcellular compartments (*4*, *5*). Identification of these individual GLUT4 compartments and assignment of their roles in the GLUT4 recycling itinerary are among the essential preliminaries to understand the insulin-induced GLUT4 recruitment at the molecular level, and remain to be achieved fully (*6*, *7*).

Using a novel subcellular fractionation protocol that does not involve cell homogenization, we have recently separated three distinct GLUT4-containing intracellular membrane fractions, T, H, and L, and have shown that the GLUT4 compartment in each of these endosomal fractions (denoted G4T, G4H, and G4L, respectively) changes in response to cellular insulin treatment (*8*). Thus, in addition to the plasma membrane GLUT4 compartment (G4PM), the three endosomal GLUT4 compartments G4T, G4H, and G4L are key participants in GLUT4 recycling and insulin-induced GLUT4 recruitment (*8*). These observations have provided compelling support for the use of a four-compartment model in the kinetic analysis of the GLUT4 recycling in rat adipocytes.

An appropriate kinetic analysis should reveal the relative contribution of each of the individual steps and compartments involved in GLUT4 recycling to the insulin-induced GLUT4

† This work was supported in part by American Diabetes Association, NIH RO1 DK13376, and Buffalo VA Medical Center Medical Research. W.L. was supported in part by American Diabetes Association Mentor-Based Fellowship Award.

* Corresponding author. Address: Biophysics Laboratory, VA Medical Center, 3495 Bailey Avenue, Buffalo, NY 14215. Tel: (716) 862-6540. Fax: (716) 862-6526. E-mail: cyjung@acsu.buffalo.edu.

‡ Present address: Ewha University, School of Medicine, Seoul, Korea.

§ Present address: Dongguk University, School of Medicine, Kyungju, Korea.

[1] Abbreviations: GLUT4, glucose transporter type 4; GLUT1, glucose transporter type 1; PM, plasma membranes; SDS-PAGE, sodium dodecyl sulfate polyacryl amide gel electrophoresis; T, trapped endosomes; H, heavy release endosomes; L, light-released endosomes; SR, sorting endosomes; ST, GLUT4-storage compartment; EV, GLUT4 exocytic vesicles. OKA, okadaic acid.

10.1021/bi026474n CCC: $22.00
Published on Web 11/02/2002

recruitment (*9*). Indeed, analysis based on a simple, four-compartment kinetic model has revealed that insulin-induced GLUT4 recruitment is associated with modulation to various extent, not only in the GLUT4 exocytosis and endocytosis steps, but also in two separate inter-endosomal trafficking steps (*9*), suggesting that insulin modulates GLUT4 recycling through multiple, compartment-specific molecular processes. The model upon which this analysis was based assumes that GLUT4 recycles from PM through SR, ST, and EV and then back to PM in that order, with first-order unidirectional transitions from one compartment to the next (*8*, *9*).

Kinetic coefficients assigned to this model were based on values of the steady-state compartment sizes of the endosomal GLUT4 compartments G4T, G4H, and G4L as well as that of G4PM measured experimentally in both the basal and insulin-stimulated states, all expressed as percentages of the total GLUT4 in the assay sample. Based in part upon heuristic considerations, G4T has been assigned to the model compartment SR, G4H to ST, and G4L to EV, thereby provisionally asserting the sequence of progression of GLUT4 through the three intracellular compartments determined experimentally. The steady-state compartment distributions obtained from the assay procedure provides sufficient information to estimate relative rate coefficients for each of the four intercompartmental steps, within the context of the proposed model structure and assumed analogy to the experimental system. Evaluation of absolute values of the rate coefficients, however, hinges upon transient data. These values have been estimated by adjusting half-times of the PM compartment relaxation in model simulations to match the corresponding experimentally obtained half-times as reported in the literature and summarized in our previous publication (*9*).

In the absence of data concerning the time dependent changes in the contents of the three intracellular compartments, however, several important questions remained unanswered with regard to the validity of the assumed model structure as an adequate representation of the cellular trafficking system. For example, is the T fraction of the assay procedure the compartment into which GLUT4 endocytosed from the plasma membrane initially flows, as implied by its assignment to the model's SR compartment? Is the basic topology of the model, an unbranched cyclic structure, consistent with the experimentally observed behavior of the GLUT4 distribution under various experimental conditions? Resolving such questions is beyond the realm of only steady-state distribution data and requires transient measurements of the individual internal compartments.

Here, we show such transient measurements in the specific case of the relaxation of the insulin-stimulated system back into the basal state. These data have proven to be quite useful in resolving the questions posed above. Most notably, it provides compelling support to our assignment of G4T to sorting endosomes in our kinetic model. In addition, the model is used to identify the kinetic basis for the insulin-like GLUT4 recruitment induced by okadaic acid (OKA) (*10*), a specific inhibitor of serine/threonine protein phosphatase PP-1 and PP-2A, in basal adipocytes. OKA is found to be as effective as insulin in enhancing the endosomal GLUT4 transition rate constants, but significantly less effective in modulating both the endocytosis and exocytosis steps of GLUT4 recycling.

MATERIALS AND METHODS

Materials. Collagenase (Type I) was obtained from Worthington (Freehold, NJ). 1F8, a monoclonal GLUT4-specific antibody, was purchased from Biogenesis Ltd. (Sandown, NH). Horseradish peroxidase-labeled protein A and anti-mouse IgG were from Zymed Laboratories (San Francisco, CA). Trisacryl beads (Reacti-Gel GF-2000) were from Pierce (Rockford, IL). All other reagents were from Sigma.

Subcellular Fractionation of Adipocytes. Isolation of adipocytes from epididymal fat pads of male Sprague−Dawley rats, the separation of the subcellular membrane fractions 900 g, 185 000 g, H, and L after hypotonic lysis, and glycerol density gradient sedimentation were carried out exactly as described (*8*). Subcellular fractionation of adipocyte homogenates into the plasma membrane-enriched fraction (PM), and the post-plasma membrane microsomal fraction (PPM) was carried out by differential centrifugation as described (*10*).

Insulin Removal and Transition Time Course Measurement. The time course of changes in the subcellular distribution of GLUT4 in intact adipocytes from the insulin-stimulated state to the basal state was followed by resuspending insulin-treated adipocytes in insulin-free suspension medium for a varying time period prior to hypotonic lysis at 4−7 °C in the presence of 2 mM KCN and 2 mM *N*-ethylmaleimide. Fresh adipocytes prepared from 30 rats (170−190 g body weights) were incubated with 10 nM insulin for 30 min at 37 °C and subsequently recovered from the incubation medium by flotation. The experimental cell sample was then resuspended into a 10-fold excess volume of prewarmed (37 °C) insulin-free buffer at time zero. After incubation in insulin-free medium with gentle mixing for the specified period of time, the medium was removed, and the cells were rapidly re-suspended into a 4-fold excess volume of prechilled (4−7 °C) insulin-free buffer containing 2 mM KCN and 2 mM NEM. This cell suspension was divided into two portions, with two-thirds being subjected to hypotonic lysis to prepare 900 g, H, and L fractions, while the remainder was simultaneously homogenized for PM and post-PM subfractionation, all at 4−7 °C in the presence of 2 mM KCN and 2 mM NEM. For each fraction and time sample, GLUT4 content was assessed in Western blots using 1F8, repeated three times using an increasing amount of sample (1/10, 1/5, and 2/5 rat equivalents for PM, 900 g, and H and 1/5, 2/5, and 3/5 rat equivalents for L). All blot intensities were quantitated by densitometry and, after correction for sample amounts, were expressed as percent of the total cellular GLUT4. In a control experiment, the insulin-stimulated cells recovered by flotation as described above were resuspended, at time zero, into a 10-fold excess volume of prechilled (4−7 °C) insulin-free buffer containing 2 mM KCN and 2 mM NEM, rather than into prewarmed (37 °C) insulin-free medium with no inhibitors. The sampling schedule and steps following the incubation periods were then exactly the same as those for the experimental sample.

Gel Electrophoresis and Immunoblotting. Solubilized membrane in Laemmli solution was applied to SDS-PAGE on 10% resolving gels and separated proteins were subjected to Western blotting using a GLUT4-specific antibody 1F8 as described (*11*). Protein bands were visualized using the enhanced chemoluminescent substrate kit (DuPont NEN),

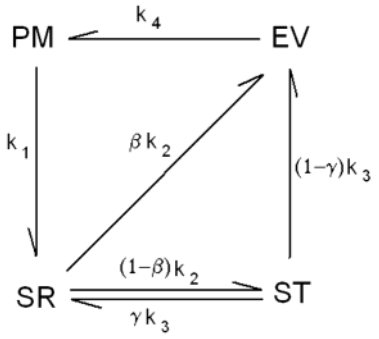

FIGURE 1: Schematic flow diagram for GLUT4 recycling model. β and γ are parameters specifying the fraction of GLUT4 moving from the sorting compartment (SR) directly into the exocytotic vesicle pool (EV), and the relative magnitude of reverse flow from the storage compartment (ST) back to SR, respectively. β, $\gamma = 0$ corresponds to the simple cyclic model analyzed earlier (9).

and immunoblot intensities were quantitated by densitometry using an analytical scanning system (Molecular Dynamics, Sunnyvale, CA). Protein was determined with the BCA kit (Pierce).

Kinetic Model. To examine the effect on system dynamics introduced by alternative pathway topography, we have formulated a generalization of the four-state model, as illustrated in Figure 1. This model is a variant of our previous model (*9*), in which we have introduced a direct pathway from the initial intracellular compartment, SR, to the exocytotic process embodied by the EV compartment. The fraction of outflow from SR taking this direct pathway is given by the parameter β, while the portion flowing into ST is proportional to $(1 - \beta)$. Thus, with β set to 0, the original conditions prevail, while at the extreme of $\beta = 1$, the model collapses into a three-compartment system, excluding ST. In a similar fashion, the parameter γ is defined as the fraction of outflow from compartment ST which returns to SR, while $(1 - \gamma)$ is the fraction transferred into the exocytotic vesicle pool, EV. Thus, as before, setting $\gamma = 0$ restores the original unidirectional cyclic model configuration. With $\gamma = 1$, ST becomes a storage compartment coupled to SR, but outside the cyclic pathway. In using this modified model to simulate transient behavior, the rate coefficients were recomputed to ensure a continued match to the observed steady-state distributions.

As in our previously published model studies (*9*), the kinetic simulations were performed using a second order predictor-corrector integration routine written in TurboBasic (Borland). Spot checks were periodically conducted using a smaller integration step size, with no discernible difference in the calculated results. The computed compartment contents were plotted as a function of time using the Axum graphing program (*12*).

RESULTS

We have shown (*8*) that hypotonic lysis followed by a low-speed centrifugation produces delipidated adipocytes as a 900 g pellet, while a high-speed centrifugation of the 900 g supernatant yields plasma membrane-free endosomes released by hypotonic lysis as a 185 000 g pellet. The endosomes in this pellet are further separated into heavy (H) and light (L) endosomes upon glycerol density sedimentation. The 900 g pellet (referred to as 900 g fraction hereafter) contained significantly more GLUT4 than expected in PM alone (*8*), indicating the presence of a endosomal pool (T) trapped within the plasma membrane sheets in 900 g and containing a significant quantity of GLUT4. Physical separation of T and PM in the 900 g fraction is not yet possible, and GLUT4 in the T fraction can be assessed only indirectly as the difference between the GLUT4 contents of 900 g and the parallel measurement of the PM-enriched fraction obtained after homogenization. The GLUT4 contents of the 900 g, H, and L fractions are expressed as percent of the total lysate GLUT4; similarly, the content of the PM-enriched fraction is given as the percent of total GLUT4 in the homogenate (PM + post-PM).

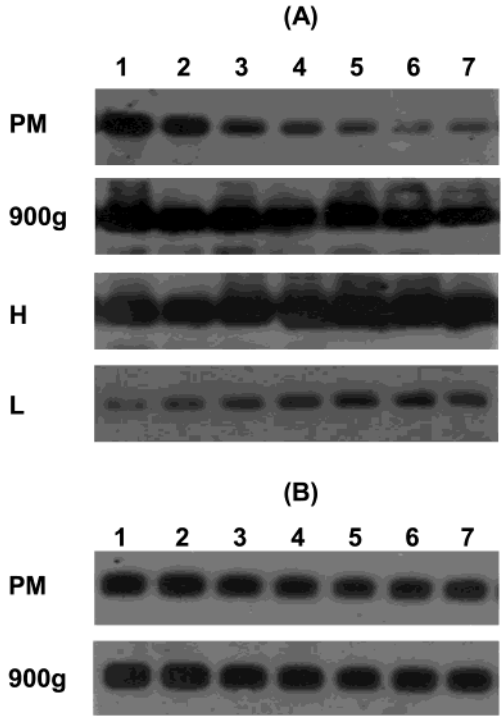

FIGURE 2: Changes in the GLUT4 immunoreactivities of PM, 900 g, H and L fractions in rat adipocytes during insulin-stimulated to basal transition. (A) Insulin-stimulated cells incubated at 37 °C in insulin-free medium for specified time periods. (B) Cells incubated at 4 °C in the presence of 2 mM KCN and 2 mM NEM (see Materials and Methods). Lanes represent incubation times of 0 (lane 1), 1 (lane 2), 3 (lane 3), 5 (lane 4), 7 (lane 5), 11 (lane 6), and 16 (lane 7) min.

Transient changes in the GLUT4 contents of four subcellular fractions were measured over a 16 min period during transition from the insulin-stimulated state to the basal state in rat adipocytes. Results of time-dependent changes in GLUT4 contents revealed in GLUT4 Western blots of PM, 900 g, H, and L fractions are illustrated in Figure 2, panel A. Several points should be noted. The insulin-stimulated steady-state PM GLUT4 compartment size (37% of total cellular GLUT4) and its time-dependent reduction upon insulin removal closely reproduce published results (summarized in ref 9), declining to 6% within 16 min, a value identical to the basal steady-state PM GLUT4 previously reported (*9*). This change in PM GLUT4 content is accompanied by characteristic increases in the GLUT4 content of the 900 g, H, and L fractions.

The accuracy of the time course thus obtained critically depends on the instantaneous arrest of GLUT4 recycling in

Table 1: Summary of Transient Changes in Four Individual GLUT4 Subcellular Compartments during the Transition from the Insulin-Stimulated State to the Basal State in Rat Adipocytes[a]

	(%)						
time (min)	0	1	3	5	7	11	16
900 g	55.9 (1.4)	54.1 (0.4)	47.6 (1.2)	40.5 (1.3)	36.8 (1.3)	31.3 (1.2)	28.1 (1.0)
G4PM	37.9 (0.3)	28.0 (0.2)	12.0 (0.3)	9.1 (0.3)	8.0 (0.1)	5.2 (0.1)	4.9 (0.1)
G4T	18.0 (1.6)	26.1 (0.3)	35.6 (1.1)	31.4 (1.1)	28.8 (1.3)	26.1 (1.2)	23.2 (1.0)
G4H	42.0 (0.3)	42.3 (0.3)	44.8 (0.1)	50.9 (0.2)	53.6 (0.4)	56.7 (0.4)	59.5 (1.5)
G4L	2.1 (0.2)	3.5 (0.1)	7.7 (0.1)	8.0 (0.2)	9.1 (0.1)	12.2 (0.2)	13.0 (0.5)

[a] The GLUT4 contents in PM, 900 g, H, and L fractions were quantified from the data of relative GLUT4 blotting intensities typified by Figure 2. For each fraction, GLUT4 blotting was repeated three times, applying an increasing amount of sample per lane (1/10, 1/5, and 2/5 rat equivalents for PM, 900 g, and H and 1/5, 2/5, and 3/5 rat equivalents for L). All blot intensities were quantitated by densitometry, and after correction for sample amounts, were expressed as percent of the total cellular GLUT4. The total cellular GLUT4 used for 900 g, H, and L data calculation was the sum of their GLUT4 blotting intensities. The total cellular GLUT4 for the PM data was obtained as the sum of the GLUT4 blotting intensities of PM and post-PM fractions of the homogenates measured in parallel. Percent distribution of GLUT4 in fraction T is calculated as the difference between the GLUT4 contents in the 900 g and the PM-enriched fractions, both expressed in percent of total cellular GLUT4. Average values are shown with the standard deviations in parentheses.

the cell at each sampling point. These transient changes were not observed in a control experiment in which the stimulated adipocytes were subjected to the insulin-free incubation at a cold temperature (4−7 °C) in the presence of 2 mM KCN and NEM (Figure 2, panel B). This result clearly demonstrates the effectiveness of the low temperature in combination with these inhibitors in arresting GLUT4 recycling at each time point.

GLUT4 levels in PM-enriched fraction as well as in 900 g, H, and L fractions were quantitated from relative GLUT4 blot intensities measured by densitometry and expressed as percent of total cellular GLUT4. Fraction T content is calculated as the difference between GLUT4 levels in 900 g and the PM-enriched fractions. These analyses are summarized in Table 1. The early rise and overshoot of G4T is apparent in the data, in contrast to the monotonic changes of the other GLUT4 compartments.

Figure 3a shows the comparison between the model simulation (curves) and the experimental results from Table 1 (discrete points) for each of the four compartments. These simulated curves are identical to those published in the earlier report (*9*), and it is worth noting that no parameters were adjusted to achieve the agreement with experimental data illustrated by Figure 3a. Note that the simulated time course of SR shows a distinct overshoot, as one would expect from the identification of this compartment with G4T.

To illustrate the effect of an alternative recycling sequence, the reverse assignment of compartments is shown in Figure 3b; namely, the T fraction is assigned to the storage compartment (ST), while the H assay fraction is interpreted as the initial intracellular compartment denoted SR in the model. The disparity between experimental observations and the model simulation is apparent.

Finally, the changes in the dynamic behavior of the original model system resulting from setting the parameters β, γ, or both to nonzero values are illustrated in Figure 4a−d. The temporal behavior of the extreme case of $\gamma = 1$, in which ST is removed from the cyclic pathway, is displayed in Figure 4e,f. Under these conditions also, the computed curves diverge significantly from the experimental data.

We next analyzed the effects of OKA, an inhibitor specific to PP-1 and PP-2A, on the GLUT4 recycling of basal adipocytes based on the four-compartment model supported above. Rat adipocytes were incubated without (basal state) and with OKA (1 μM) or with insulin (10 nM) for 30 min

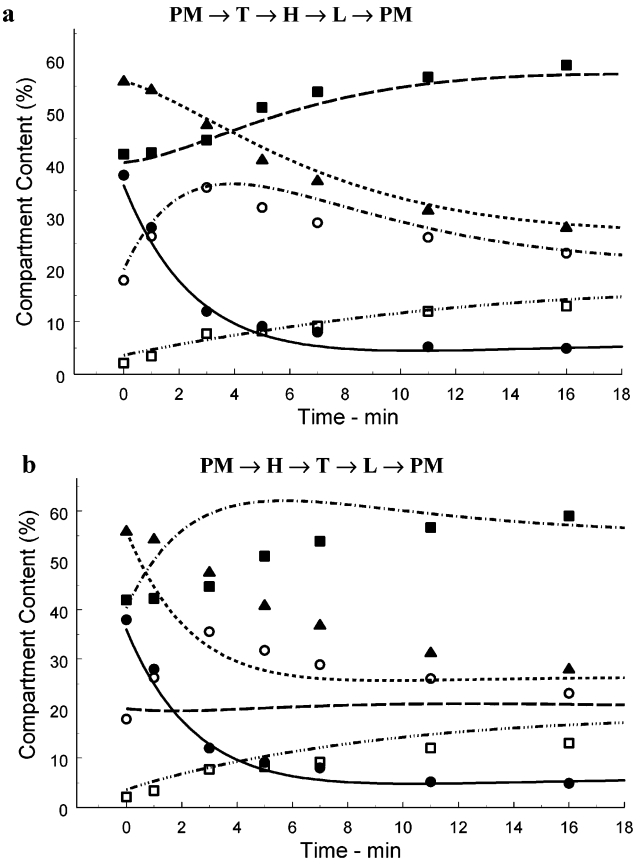

FIGURE 3: Experimental data (symbols) compared with simulated results (continuous curves), with β and $\gamma = 0$. Symbol key: ● G4PM, □ G4L, — PM, -•••- EV, ○ G4T, ▲ 900 g, —•— SR, --- 900 g, ■ G4H, − − − ST. (a) Model (with T assigned to SR, H to ST) is identical to that presented before (*9*) and uses kinetic coefficients from the earlier analysis. Excepting that shown in **3b**, all models presented are based upon this sequence assignment, and in each the curve labeled 900 g is computed as PM + SR. (b) Model with sequence reversed (T assigned to ST, H to SR) showing a marked lack of congruence between experimental and simulated results. In this case only, the continuous curve denoted 900 g is computed as PM + ST.

at 37 ° C and used to prepare 900 g, H, and L fractions by hypotonic lysis protocol and PM and PPM fractions by homogenation protocol. The GLUT4 distribution among these fractions was measured by GLUT4 immunoblot (Figure 5). Like insulin, OKA clearly increased the GLUT4 content in PM but to a lesser extent than insulin (Figure 5A),

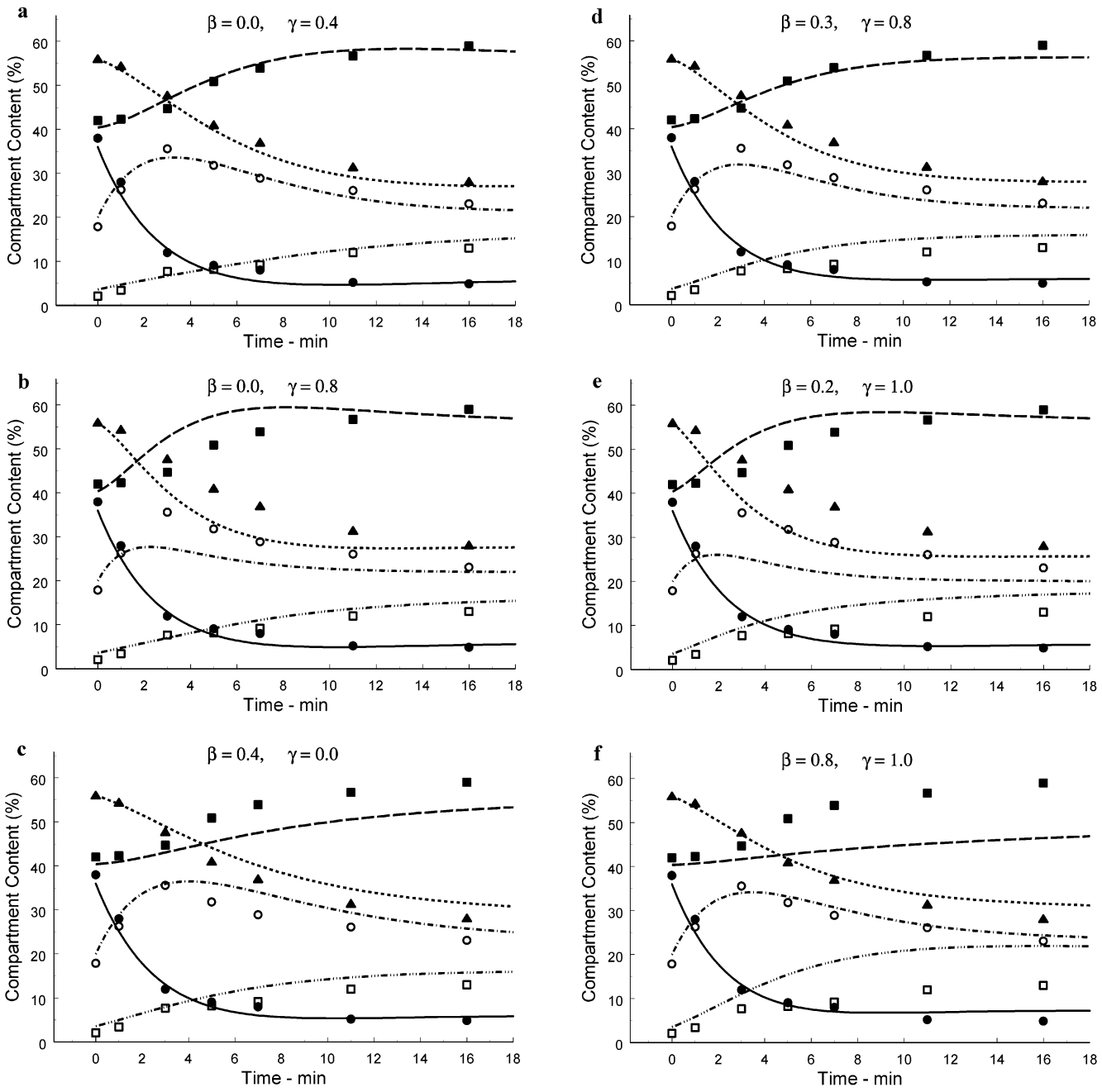

FIGURE 4: Experimental data (symbols) compared with simulated results (continuous curves) of the model (Figure 1), for various values of the parameters β and γ, as indicated. Symbol and line assignments are: ● G4PM, □ G4L, — PM, -···- EV, ○ G4T, ▲ 900 g, —·—· SR, --- 900 g, ■ G4H, — — — ST. In each case, the 900 g curve corresponds to PM + SR.

reproducing previous findings (10). OKA also mimicked insulin in increasing GLUT4 in 900 g and reducing GLUT4 in H and L fractions (Figure 5B) although OKA was quantitatively less effective compared to insulin (Figure 5B). The difference is most drastic in the L fraction, as revealed in glycerol gradient sedimentation (Figure 6). Relative GLUT4 distributions among PM, T, H, and L were expressed in percents of the total cellular GLUT4 content (Table 2). Note that OKA reduced GLUT4 in L only by 24% compared to a more than 3-fold reduction by insulin.

The steady-state GLUT4 compartment sizes assessed above give the relative magnitudes of the four rate coefficients, k_1, k_2, k_3, and k_4 as defined in Figure 1 (with $\beta = 0$ and $\gamma = 0$; see below). The absolute values of the coefficients were then calculated from the time dependent (transient) behavior of the model. By scaling the sets of rate coefficients, such that the experimentally observed and simulated time constants of the plasma membrane content are as similar as possible, absolute values can be assigned to the rate coefficients. Independent scaling factors are employed in the cases of basal conditions, insulin-, and OKA-stimulated cells.

The effect of OKA in modulating the kinetic coefficients, evaluated with reference to the unbranched cyclic model ($\beta = 0$, $\gamma = 0$), is also shown in Table 2. Rate coefficients found in the instance of basal state cells, and under insulin stimulation, in addition to those found in the presence of OKA are presented. For comparison, the corresponding exocytosis rate constants, k_{ex}, computed using a two-compartment model (*3*), are also shown. The transient parameter values $t_{1/2}$ (*3*) given in the table are the relaxation

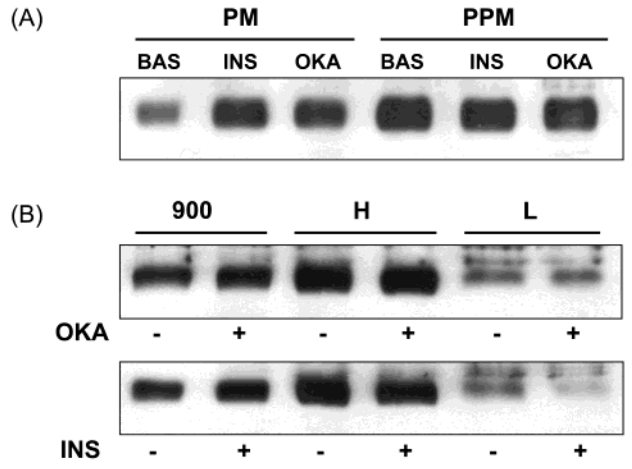

FIGURE 5: Subcellular distribution of GLUT4 in adipocytes without (BAS) and with insulin (INS) and OKA (OKA) treatmentas assessed by GLUT4 blotting. PM and PPM were separated from homogenates and 900 g; H and L were prepared from hypotonic lysates as described in Materials and Methods. A fixed portion of each fraction was loaded on each lane. The data shown are representative of three independent experiments.

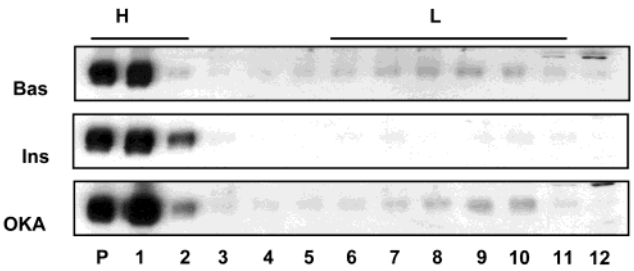

FIGURE 6: GLUT4 distributions in H and L fractions obtained by glycerol density sedimentation. 185 000 g pellets were prepared from hypotonic lysates of adipocytes without (BAS) and after insulin (INS) or OKA (OKA) treatment and subjected to glycerol gradient fractionation. Fractions were collected from the bottom to the top (P and fractions 1−12) as described (*8*). A fixed portion of each fraction was loaded on each lane for GLUT4 blotting. The results were reproduced in three other experiments.

half-times experimentally determined for the GLUT4 plasma membrane pool and are the basis for assigning absolute values to the rate coefficients as discussed (see above).

With reference to the results shown in Table 2, it can be seen that both OKA and insulin treatments reduce k_1 while increasing k_2, k_3, and k_4. Significantly, however, insulin is much more (>2-fold) effective in increasing k_4 and reducing k_1. On the other hand, OKA is equally or more effective than insulin in increasing k_2 and k_3. Thus, OKA fully reproduces the insulin action on the GLUT4 endosomal trafficking processes but only partially reproduces the insulin effect on k_1 and particularly the major insulin-sensitive step, suggesting the involvement of a mechanism in addition to the OKA-sensitive one in this step.

DISCUSSION

Support for the Presumptive GLUT4 Itinerary Sequence. Ideally the results presented here will be supplemented by additional repetitions of this experiment and measurements made under the complementary conditions of relaxation from the basal into the insulin-stimulated state. Nonetheless, the results conform surprisingly well to the time course previously computed from model simulations without the need for further adjustment of kinetic parameters. In light of this experimental kinetic data and its comparison with simulated model results, we can make the following observations concerning the questions raised in the Introduction, particularly with regard to the position of the T fraction in the recycling itinerary of GLUT4:

1. Compartment Sequence. The overshoot in the time course of the T fraction (and SR in the model) as seen in Figure 3a would suggest intuitively that this compartment is sequentially adjacent to the plasma membrane, since initially PM is the only compartment at a significantly higher value than its ultimate steady state value. This argument can be made more rigorous by focusing upon conditions at the time of the maximum in G4T. At that instant, the rate of flow into T is precisely balanced by the outflow. Since the content of the T fraction is about 50% larger than its basal steady state level, the outflow (be it to one or more compartments) must also exceed its final steady state magnitude by 50%. Correspondingly, the inflow rate must then also be 1.5 times its basal steady value, requiring that some compartment feeding T have a content at least 50% larger than its final value. Inspection of the data shows that PM is the only compartment satisfying this condition. Consequently, regardless of the pathway configuration of the recycling system, the T fraction must be directly downstream from the plasma membrane.

The comparison case, with the assumed sequence of the T and H fractions reversed in the GLUT4 cycling itinerary, results in a much poorer correlation of experiment and simulation, as shown in Figure 3b. There is no discernible overshoot of the model's ST compartment corresponding to that observed in the T fraction. In addition, the increase in G4H found experimentally is much slower than the simulated rise in SR, and a slight overshoot in the model compartment can be seen.

The interpretation of G4L as exocytotic vesicles is completely consistent with the experimental findings, as evidenced by the close correspondence to the simulation. The possibility of some contribution to this fraction by interendosomal vesicles or endocytotic vesicles cannot be excluded. The late temporal rise in this fraction, however, would indicate that any such contribution from processes earlier in the recycling pathway must be relatively small in magnitude.

2. Model Topography. It is certainly a possibility that an alternative arrangement of pathways among the four compartments of the model more closely represents the physical system (*13*−*15*). This would be a difficult issue to explore in the absence of transient experimental data such as that presented here. We consider only four-compartment models since a more complex system of more compartments is not likely to be distinguishable, given the experimental variation of available data. Additionally, four is the number of compartments separately measured by the experimental assay procedure. Hence it is recognized from the onset that a four-compartment representation very probably involves lumping together of theoretically distinct compartments in a system much more complex in reality.

Figure 4a−d displays the behavior of the models altered by allowing direct transition from SR to EV ($\beta \neq 0$) and the reverse flow from ST to SR ($\gamma \neq 0$) according to the flowchart of Figure 1. As is apparent from these plots, the changes in the time courses of distributions among the

Table 2: Effects of OKA and Insulin on GLUT4 Steady-State Compartment Sizes and Calculated Rate Constants[a]

compartments	units	BAS	INS	OKA	INS/BAS	OKA/BAS	OKA/INS
PM	%	5.0 (0.45)	32.6 (2.54)	20.9 (0.92)	6.52	4.18	0.64
T	%	19.8 (1.20)	18.9 (1.09)	14.5 (1.02)	0.95	0.78	0.77
H	%	57.0 (3.01)	43.4 (3.12)	50.7 (2.97)	0.76	0.89	1.17
L	%	18.2 (1.09)	5.1 (0.40)	13.9 (0.78)	0.28	0.76	2.73
$t_{1/2}$	min	1.7	3.3	2.1			
k_1	min^{-1}	0.380	0.124	0.240	0.33	0.63	1.94
k_2	min^{-1}	0.096	0.124	0.346	2.23	3.61	1.62
k_3	min^{-1}	0.033	0.093	0.099	2.79	2.97	1.06
k_4	min^{-1}	0.104	0.793	0.361	7.59	3.46	0.46
k_{ex}	min^{-1}	0.020	0.060	0.063	3.00	3.17	1.06
J	(% min^{-1})	1.90	4.04	5.02	2.13	2.64	1.24

[a] Steady-state compartment sizes measured in basal (BAS), insulin-stimulated (INS), and OKA (OKA)-treated rat adipocytes as illustrated in Figure 5. Values represent averages of 3−4 measurements with the standard deviation in parentheses. Kinetic rate coefficients k_1, k_2, k_3, and k_4 are computed upon the basis of the circular four-compartment model shown in Figure 1 with β and $\gamma = 0$. These steady-state pool sizes establish relative values of the rate coefficients. An estimate of absolute values is obtained by matching the simulated transient behavior to the half-times ($t_{1/2}$) observed experimentally (see ref *9*). The rightmost three columns are the ratios of the pool sizes or parameter values in two cell states, as indicated in the header. The parameter k_{ex} is the corresponding exocytotic rate coefficient resulting from a two-compartment model treatment. J is the computed flux rate for the circulation of GLUT4 through the recycling pathway (*9*).

compartments is not dramatic for small values of the parameters β and γ. With $\beta = 0.4$, differences from the original model are noticeable in the slower rise of ST to its steady-state value and the more rapid rise in EV (Figure 4c). These changes are expected as a result of the introduction of a direct pathway from SR to EV, at the expense of flow into ST. On the other hand, introducing a reverse process from ST back to SR ($\gamma = 0.4$, $\beta = 0$), as shown in Figure 4a, seems to very slightly improve the fit between the experimental data and theoretical curves. Increasing the parameter γ to 0.8, however, causes a marked decrease in the peak level attained by SR and a more rapid rise in ST content toward its steady state level (Figure 4b). These changes are also easily understood when it is recalled that the forward rate coefficient linking SR and ST (k_2) must be increased to compensate the reverse flux in order to maintain the observed steady-state distribution. It is also interesting to note that the alterations introduced by β and γ independently are, to some extent, compensatory. Thus, the curves resulting from $\beta = 0.3$ and $\gamma = 0.8$, shown in Figure 4d, are very similar to those of the unmodified model (Figure 3a).

In the case of $\gamma = 1$, ST becomes a dead-end compartment, coupled with SR but removed from the cyclic pathway. The role of β then becomes that of setting the relative kinetics of flow from SR to ST and back, and from SR to EV in the cycling itinerary. From the behavior shown in Figure 4e,f, our experimental data indicate that this model structure, $\gamma = 1$, is unlikely. With $\beta = 0.2$, for example, the computed SR compartment has a much smaller overshoot than that found in G4T. With $\beta = 0.8$, the rate of increase in ST is much less than observed in the corresponding experimental fraction, while the reverse is true of the EV compartment. Consequently, on the basis of these results, we are confident in excluding this extreme case as a likely possibility. There is, however, a rather broad intermediate range of values of β and γ in which the computed results are close to the measured values, and given the experimental variability of the data, systems within this range cannot be excluded as feasible representations of reality.

Evidence suggests that GLUT4 may recycle through a constitutive pathway involving the recycling endosome as well as through the specific insulin-regulated pathway incorporating the putative GLUT4-specific storage endosome (*16*−*19*). These two pathways are seemingly differentially affected by various inhibitors and stimulators (*20*−*22*). In future studies, an exploration of the effects of these modulating agents may reveal a more richly detailed topology of the GLUT4 recycling pathway. On the basis of the present data, however, the values for β and γ have not been shown to deviate significantly from zero, and elaboration of the simple linear GLUT4 pathway originally proposed does not appear to be warranted.

3. Implication for the GLUT4 Trafficking Pathway. The experimental findings of this study represent the first reported set of directly measured changes in each of the four distinct GLUT4 compartment sizes during the transition between insulin-stimulated and basal states in rat adipocytes. As such, it provides information, which would otherwise be inaccessible, concerning the kinetics and topography of the GLUT4 recycling pathway. Most significantly, it provides compelling experimental evidence that the GLUT4 compartment in the T fraction (G4T) is directly downstream from the PM in the recycling sequence, representing the early (or sorting) endosome (*23*), while the GLUT4 compartment in the H fraction (G4H) is later in the sequential order of GLUT4 cycling.

One may also conclude from these studies that a four-compartment model in which ST is a dead-end storage compartment, coupled to but outside the recycling pathway ($\gamma = 1$), is inconsistent with the experimentally measured transient data. On the other hand, some degree of backflow from ST to SR (γ small but nonzero) cannot be excluded. Similarly, some fraction, probably no more than 30%, of the recycling GLUT4 traffic may flow from SR directly to the exocytotic vesicle pool. Nonetheless, the original model ($\beta = 0$, $\gamma = 0$) proves to be adequate to reproduce the experimental findings at the present time.

Significance of Endosomal Trafficking Processes to GLUT4 Exocytosis. In earlier studies (*3*, *10*), the inability to differentially assess individual endosomal GLUT4 compartments allowed us only to analyze the kinetics of the GLUT4 recycling on the basis of a two-compartment model composed of the plasma membrane pool and an undifferentiated

intracellular compartment, characterized by two first-order kinetic coefficients, an endocytotic rate k_{in}, and a rate constant associated with the exocytosis process returning GLUT4 from the interior to the plasma membrane, k_{ex}. Such an analysis using data obtained from rat adipocytes showed that insulin affects both k_{ex} and k_{in}, while OKA affects primarily k_{ex}. In comparison, Table 2 demonstrates the major effect of OKA to be exerted upon k_2 and k_3, with a considerably smaller effect than insulin upon k_4, even though both agents produce a similar value for k_{ex}.

It is instructive, therefore, to analyze the relationship between the rate coefficients of the two-compartment model and the present model comprising four compartments. In both treatments, the flux of GLUT4 in the recycling pathway is proportional to the plasma membrane pool, with k_{in} and k_1 as the proportionality coefficients in the two- and four-compartment models, respectively. It is apparent that these rate coefficients are equivalent.

In the two-compartment model, the recycling flux rate, denoted J, is given by the product k_{ex} $G4_{intra}$, in which the total intracellular amount of GLUT4 ($G4_{intra}$) is equal to the sum of the intracellular compartment contents in the four-compartment model. That is

$$G4_{intra} = SR + ST + EV \quad (1)$$

Each of the compartment sizes can be expressed in terms of the flux, J, by observing that

$$G4_{intra} = J/k_{ex}; \qquad SR = J/k_2; \qquad \text{etc.} \quad (2)$$

Simple rearrangement of these relations leads to the desired relationship:

$$1/k_{ex} = 1/k_2 + 1/k_3 + 1/k_4 \quad (3)$$

Thus, if the reciprocal rate coefficient is viewed as the "resistance" of that process, the lumped resistance of exocytosis in the two-compartment model is merely the sum of the resistances of the two intracellular processes and the exocytotic step in the four-compartment configuration.

Both OKA and insulin modulate each of the four rate constants of GLUT4 trafficking, reducing k_1 and increasing k_2, k_3, and k_4 (Table 2). Significantly, OKA is notably less effective than insulin in modulating k_1 and k_4, the rate constants involved with entering or leaving the plasma membrane. On the other hand, it is equally or more effective in the modulation of k_2 and k_3, the two rate constants associated with the endosomal system. These findings with OKA suggest that the states of protein phosphorylation most likely involving certain protein kinases and/or phosphatases in a compartment-specific manner, play key roles in insulin-induced GLUT4 recruitment in rat adipocytes at all of the transition processes including those between endosomal compartments.

REFERENCES

1. Cushman, S. W., and Wardzala, L. J. (1980). Potential mechanism of insulin action on glucose transport in the isolated rat adipose cells: Apparent translocation of intracellular glucose transport systems to the plasma membrane, *J. Biol. Chem. 255*, 4758−4762.
2. Suzuki, K., and Kono, T. (1980). Evidence that insulin causes translocation of glucose transport activity to the plasma membrane from an intracellular storage site, *Proc. Natl. Acad. Sci. U.S.A. 77*, 2542−2545.
3. Jhun, B. H., Rampal, A. L., Liu, H. Z., Lachaal, M., and Jung, C. Y. (1992). Effects of insulin on steady-state kinetics of GLUT4 subcellular distribution in rat adipocytes. Evidence of constitutive GLUT4 recycling, *J. Biol. Chem. 267*, 17710−17715.
4. Malide, D., Dwyer, N. K., Blanchette-Mackie, E. J., and Cushman, S. W. (1997). Immunocytochemical evidence that GLUT4 resides in a specialized translocation post-endosomal VAMP2-positive compartment in rat adipose cells in the absence of insulin, *J. Histochem. Cytochem. 45*, 1083−1096.
5. Simpson, F., Whitehead, J. P., and James, D. E. (2001) GLUT4 at the cross roads between membrane trafficking and signal transduction, *Traffic 2*, 2−11.
6. Holman, G. D., Sandoval, I. V. (2001). Moving the insulin-regulated glucose transporter GLUT4 in to and out of storage, *Trends Cell Biol. 11*, 173−179, Review.
7. Martin, S., Millar, C. A., Lyttle, C. T., Meerloo, T., Marsh, B. J., Gould, G. W., and James, D. E. (2000). Effects of insulin on intracellular GLUT4 vesicles in adipocytes: evidence for a secretory mode of regulation, *J. Cell Sci. 113*, 3427−3438.
8. Lee, W., Ryu, J., Souto, R. P., Pilch, P. F., and Jung, C. Y. (1999). Separation and partial characterization of three distinct intracellular GLUT4 compartments in rat adipocytes: Subcellular fractionation without homogenization, *J. Biol. Chem. 274*, 37755−37762.
9. Lee, W., Ryu, J. W., Spangler, R. A., and Jung, C. Y. (2000). Modulation of GLUT4 and GLUT1 recycling by insulin in rat adipocytes: Kinetic analysis based on the involvement of multiple intracellular compartments, *Biochemistry 39*, 9358−9366.
10. Rampal, A. L., Jhun, B. H., Kim, S., Liu, H., Manka, M., Lachaal, M., Spangler, R. A., and Jung, C. Y. (1995) Okadaic acid stimulates glucose transport in rat adipocytes by increasing the externalization rate constant of GLUT4 recycling, *J. Biol. Chem. 270*, 3938−3943.
11. Jhun, B. H., Hah J. S., and Jung C. Y. (1991). Phenylarsine oxide causes an insulin-dependent, GLUT4-specific degradation in rat adipocytes, *J. Biol. Chem. 266*, 22260−22265.
12. MathSoft, Inc. (1996) *AXUM*, ver. 5.0A, Cambridge, MA.
13. Holman, G. D., Lo Leggio, L., and Cushman, S. W. (1994). Insulin-stimulated GLUT4 glucose transporter recycling. A problem in membrane protein subcellular trafficking through multiple pools, *J. Biol. Chem. 269*, 17516−17524.
14. Yeh, J. I., Verhey, K. J., and Birnbaum, M. J. (1995). Kinetic analysis of glucose transporter trafficking in fibroblasts and adipocytes, *Biochemistry 34*, 15523−15531.
15. Pessin, J. E., Thurmond, D. C., Elmendorf, J. S., Coker, K. J., and Okada, S. (1999) Molecular basis of insulin-stimulated GLUT4 vesicle trafficking. Location! Location! Location! *J. Biol. Chem. 274*, 2593−2596.
16. Martin, S., Tellam, J., Livingstone, C., Slot, J. W., Gould, G. W., James, and D. E. (1996). The glucose transporter (GLUT-4) and vesicle-associated membrane protein-2 (VAMP-2) are segregated from recycling endosomes in insulin-sensitive cells, *J. Cell Biol. 134*, 625−635.
17. Rea, S., and James, D. E. (1997). Perspectives in diabetes: Moving GLUT4; The biogenesis and trafficking of GLUT4 storage vesicles, *Diabetes 46*, 1667−1677.
18. Kandror, K. V., and Pilch, P. F. (1998) Multiple endosomal recycling pathways in rat adipose cells, *Biochem. J. 331* (Pt3), 829−835.
19. Martin, S., Millar, C. A., Lyttle, C. T., Meerioo, T., Marsh, B. J., Gould, G. W., and James, D. E. (2000). Effects of insulin on intracellular GLUT4 vesices in adipocytes: evidence for a secretory mode of regulation, *J. Cell Sci. 113*, 3427−3438.
20. Holman, G. D., and Sandoval, I. V. (2001). Moving the insulin-regulated glucose transporter GLUT4 in to and out of storage, *Trends Cell Biol. 11*, 173−179.
21. Robinson, L. J., Pang, S., Harris, D. S., Heuser, J., and James, D. E. (1992). Translocation of the glucose transporter (GLUT4) to the cell surface in permeabilized 3T3-L1 adipocyutes: effects of ATP, Insulin and GTPγS and Localization of GLUT4 to clathrin lattices, *J. Cell Biol. 117*, 1181−1196.
22. , Lalioti, V., Vergarajauregui, S., and Sandoval, I. V. (2001). Targeting motifs in GLUT4 (Review), *Mol. Membr. Biol. 18*, 257−264.
23. Mukherjee, S., Ghosh, R. N., and Maxfield, F. R. (1997) *Endocytosis, Physiol Rev. 77*, 759−803.

BI026474N